Letter

BSA-Sugar Conjugates as Ideal Building Blocks for SPR-Based Glycan Biosensors

Shun Tao, Tian-Wei Jia, Yang Yang, and Li-Qiang Chu

ACS Sens., **Just Accepted Manuscript** • DOI: 10.1021/acssensors.6b00679 • Publication Date (Web): 30 Dec 2016

BSA-Sugar Conjugates as Ideal Building Blocks for SPR-Based Glycan Biosensors

Shun Tao,[a] Tian-Wei Jia,[b] Yang Yang,[b,*] and Li-Qiang Chu[a,*]

[a]College of Chemical Engineering and Materials Science, Tianjin University of Science & Technology, No.29, 13th Ave., TEDA, Tianjin 300457, China

[b]China International Science and Technology Cooperation Base of Food Nutrition/Safety and Medicinal Chemistry, Sino-French Joint Lab of Food Nutrition/Safety and Medicinal Chemistry, Key Laboratory of Industrial Fermentation Microbiology of Ministry of Education, Tianjin Key Laboratory of Industry Microbiology, College of Biotechnology, Tianjin University of Science & Technology, No.29, 13th Ave., TEDA, Tianjin 300457, China

Supporting Information

ABSTRACT: Controlled immobilization of sugar probes is of key importance for the development of glycan biosensors. To this end, a series of BSA-sugar conjugates with different number of mannose are prepared via the squaric acid-mediated coupling reaction. The conjugates can absorb directly on gold substrate without any derivation reactions, thus providing a simple and effective method for the construction of SPR-based glycan biosensors. SPR measurements show that the BSA-mannose conjugate with 11 mannoses exhibit the highest affinity to the lectin concanavalin A with a limit of detection of ca. 1.8 nM. Regeneration and specificity of the obtained glycan biosensors are also investigated.

KEYWORDS: glycan biosensor, surface plasmon resonance, BSA-sugar conjugate, mannose, concanavalin A.

Recently glycan biosensors have attracted a great deal of interest due to their wide applications in life science and biomedical fields, such as glycomics research, drug and vaccine screening, pathogen diagnosis, etc.[1, 2] Because of the multivalent nature of carbohydrate-lectin interaction,[3] the glycan probes attached onto a biosensor surface are required to have an appropriate lateral distribution and conformation, aiming at mimicking the glycocalyx on cell surfaces. While large polysaccharide probes could be easily attached onto various substrates via either hydrophobic interactions or van der Waals' force, the immobilization of small hydrophilic sugar probes (i.e., monosaccharide and disaccharide) usually rely on either the derivation of sugar molecules with functional groups (e.g., -SH, -NH_2, etc.) or the synthesis of glycoconjugates with various scaffolds, such as dendritic polymers, DNA, lipid, and so on.[4, 5] Direct coupling of unmodified small sugars onto either graphene-coated or photochemical-active surfaces were also reported recently.[6, 7] Despite extensive research, it is still highly desirable to develop a simple and effective immobilization strategy to control the lateral distribution of small sugar probes.

Proteins with desired 3D structures have approved to be useful building materials for the construction of biosensors.[8, 9] Bovine serum albumin (BSA) is the most abundant protein with relative low cost. Moreover, BSA has ca. 20 lysine residues at its outer surface and the distance between two lysines is between 2.0 and 2.4 nm,[10] which makes it a potential scaffold to control the lateral distribution of the coupled sugar probes. Therefore, in this work, we explore the synthesis and the immobilization of a series of BSA-sugar conjugates on gold substrate (as illustrated in Figure 1), and the performance of the resulting glycan biosensor is evaluated by using surface plasmon resonance spectroscopy (SPR). In this design, BSA is employed not only as a 3D scaffold to adjust the distribution of the sugar probes, but also as the anchoring group because of its strong adsorption on gold. While several research groups had reported the preparation of BSA-sugar conjugates and their applications as either carbohydrate vaccine/antibody[11, 12] or immobilization linker,[13, 14] there are few studies about its use as anchoring group directly.[15]

Figure 1a shows the schematic illustration of the synthetic procedure of BSA-mannose conjugates (see the details in the Supporting Information). Mannose (Man) was chosen as model sugar in this study because it exhibited specific recognition with concanavalin A (ConA), the most extensively studied carbohydrate-lectin pair.[16] As shown in Figure 1a, mannose was firstly modified at anomeric center with a hexylamine, which is

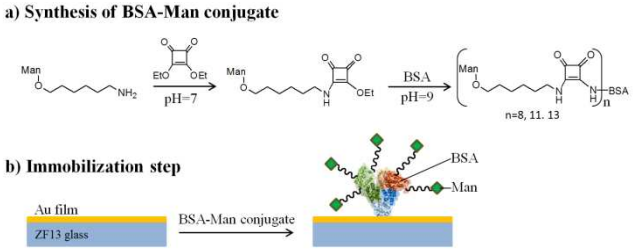

Figure 1. Schematic representation of the synthesis of BSA-Man conjugate via the squaric acid mediated coupling reaction (a), and the subsequent immobilization on gold surface via non-specific adsorption (b).

Table 1. The Characteristics of Various BSA-Man Conjugates.

Samples	BSA:Man ratio	MW	Man loading	Man spacing (nm)	Thickness (nm)	k_{on} ($\times 10^3 M^{-1}s^{-1}$)	k_{off} ($\times 10^{-4} s^{-1}$)	K_D (nM)
BSA	---	66450	0	---	3.15±0.38	---	---	---
BSA-M8	1:15	69910	8	4.4	2.40±0.24	9.6	7.4	77.1
BSA-M11	1:30	70709	11	3.8	2.07±0.27	12.3	8.5	69.3
BSA-M13	1:50	71512	13	3.5	1.86±0.13	4.5	10.9	242.2

Note: The MWs of the BSA and three BSA-Man conjugates are from MALDI-TOF-MS measurements. The average number of mannose loading was calculated from the MW of the conjugates. Spacing between two mannose probes is calculated assuming even distribution on BSA surface. The thicknesses of the adsorbed proteins on gold are from SPR measurements. The k_{on} and the k_{off} are from the fitting of the SPR kinetic measurement assuming pseudo-first-order model. The ConA's concentration is 5 μM.

assumed to improve the flexibility of the coupled mannose probes. Then it was linked with the lysine residues of BSA via the squaric acid mediated conjugation in carbonate buffer (pH=9).[17] The number of the mannose was controlled by adjusting the reaction ratio of BSA:Man from 1:15, 1:30 to 1:50. The resulting BSA-Man conjugates were characterized by using the matrix-assisted laser desorption/ionization time of flight mass spectrometry (MALDI-TOF-MS), as shown in Figure S1. The average number of the coupled mannose was calculated to be 8, 11 and 13 (see Table 1), which are referred to as BSA-M8, BSA-M11 and BSA-M13, respectively.

Several recent works show that BSA has a compact triangular conformation in the pH range 4~9 with typical dimensions of 9.2×9.2×9.2×3.0 nm.[18, 19] Thus the surface area of a BSA can be calculated to be about 156 nm^2. If assuming the mannose probes are attached evenly on BSA surface, the spacing between the probes for BSA-M8, BSA-M11 and BSA-M13 will be equal to 4.4 nm, 3.8 nm and 3.5 nm, respectively. It should be noted that the loading of mannose to BSA was not done in a site-specific manner. Moreover, BSA is classed as a soft protein,[20] meaning that the conformation of the BSA adsorbed on gold may undergo slight change. Therefore, the use of BSA as scaffold just allow for the control of the average sugar density rather than a spatially-defined arrangement.

SPR is widely accepted as a sensitive and label-free technique for the detection of protein adsorption. Thus an angle-modulated SPR setup[21, 22] was employed to measure the thickness of various BSA-Man conjugates adsorbed on gold surface. Firstly the freshly-deposited gold substrate was attached to a flow cell and PBS buffer (pH=7.4) was injected into the cell using a peristaltic pump. After several minutes for stabilization, the protein solution of 1 mg/mL was introduced into the flow cell at a flow rate of 700 μL/min. The SPR spectra (i.e., the reflectivity vs. incident angle curve) were recorded before and after the adsorption, which could be fitted using the Winspall software in order to determine the thickness of the adsorbed layers. The refractive indices of the BSA and all BSA-Man conjugates are assumed to be n=1.45.[23]

The thicknesses of various BSA-Man conjugates adsorbed on gold are given in Table 1. It can be found that the thickness of bare BSA adsorbed on gold is about 3.15± 0.38 nm. By using the de Feijter's equation,[24] the surface density of BSA can be calculated to be 203 ng/cm^2. This result suggests that a monolayer of BSA adsorbed on gold surface, which is in good agreement with the literature.[19, 22] From Table 1, one also can find that, when the number of mannose coupled to BSA increased from 8 to 11 and 13, the thicknesses of the corresponding conjugates on gold decreased from 2.40±0.24 nm to 2.07±0.27 nm and 1.86 ± 0.13 nm. The reduced adsorption of BSA-Man conjugates could be ascribed to the hydrophilic nature of mannose moiety. On the other hand, the results clearly indicate that all BSA-Man conjugates could spontaneously adsorb onto the gold, and BSA indeed can be used as anchoring group for the immobilization of sugar probes. Noted that the lower thickness of the BSA-sugar conjugate on gold as compared with that for bare BSA suggests that some parts of the gold surface may not be occupied, which may cause non-specific adsorption when in contact with target solution. Therefore, for all sensors prepared via the direct adsorption of the BSA-sugar conjugate, BSA solution of 1mg/mL was injected thereafter to form a passivation layer (see Figure S2).

The binding kinetics of ConA with the immobilized BSA-Man conjugates then were investigated by using SPR.[25, 26] When the association process reached the equilibrium, SPR spectrum was collected in order to quantify the amount of the captured ConA. After that, PBS buffer was injected again and the dissociation process takes over. NaOH of 10 mM was used to remove all captured ConA and the SPR chip could be reused for further detection, as indicated in Figure S3. This result also suggests that the immobilized BSA on gold remain stable again the regeneration solution. Prior to monitoring the binding of ConA with three BSA-Man conjugates, non-specific adsorption of ConA with pure BSA was tested, as shown in Figure S4. It is apparent that the ConA do not adsorb onto the BSA monolayer.

Figure S5 shows the SPR kinetic monitoring of various concentrations of ConA on the chips prepared with BSA-M8, BSA- M11 and BSA-M13, respectively. From Figure S5, it is apparent that a low concentration of ConA gives rise to a slow association process. Moreover, increasing the concentration would result in a fast association process Both the association constant k_{on} and dissociation constant k_{off} can be determined from the SPR kinetic curves by using the *OriginPro* software (see all fitting curves in Figure S5).[26, 27] The values of k_{on}, k_{off} and K_D at a ConA of 5 μM are given in Table 1 for three types of BSA-Man conjugates. The K_D values vary from 69.3 to 242.2 nM, and are in good agreement with the literature,[14, 27, 28]

indicating that the multivalent interactions take place for all BSA-Man conjugates regardless of the mannose density. On the other hand, the lowest K_D value is for the SPR chip with BSA-M11, suggesting that it has the highest affinity to ConA. Notice that the highest k_{off} is for the chip with BSA-M13 and the highest k_{on} is for BSA-M11. Therefore, the high affinity of the chip with BSA-M11 is mainly due to its high association constant.

By assuming that the refractive index of ConA is n=1.57,[16] the thickness of the captured ConA could be obtained by fitting the SPR spectrum. Figure 2 compared the thickness of the ConA bound to three types of chips as a function of the ConA concentration. One can find that, the thickness of ConA on the BSA-M11 chip is higher than those for BSA-8M and BSA-M13 for the whole concentration range. For instance, when in contact with 10 μM ConA for 35 mins, the chip with BSA-M11 can catch as thick as 2.97 nm of ConA, while the chips with BSA-M8 and BSA-M11 have the thickness of 2.46 and 2.02 nm, respectively. These results, associated with the aforementioned kinetic data, clearly show that BSA-M11 has the highest affinity with ConA and thus has the optimized mannose density. In contrast, either a lower (i.e., BSA-M8) or a higher (i.e., BSA-M13) number of mannose probes would result in a decreased affinity with ConA. It should be noted that the average spacing between the mannose probes for the current BSA-Man conjugates are ranging from 4.4 to 3.5 nm (see Table 1), which is higher than the a separation distance for the binding sites of ConA (i.e., 4.7 ~ 6.5 nm).[28, 29] Therefore, the results suggest that the distribution of the mannose probes on BSA indeed is not homogeneous. On the other hand, beside the mannose density, the flexibility of the sugar probes may also account for the binding of ConA.

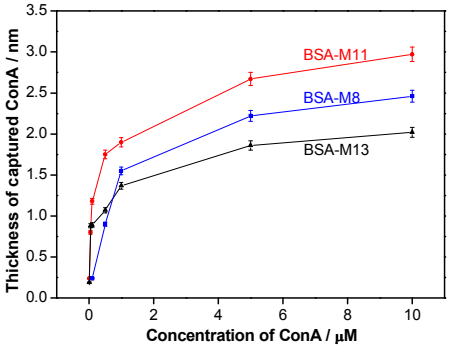

Figure 2. Comparison of the thickness of the captured ConA on various SPR chips prepared with BSA-M8, BSA-M11 and BSA-M13, respectively.

After the adsorption of 10 μM of ConA on the chip with BSA-M11, the resulting surface density of ConA can be calculated to be 387 ng/cm² using the de Feijter's equation. ConA has a MW of ca. 102 kDa with dimensions of 6.3×8.7×9.0 nm,[16, 29] and thus the surface density of a densely packed monolayer of ConA will vary from 216 to 309 ng/cm². Therefore, it appears that the BSA-M11 chip could capture more than one monolayer of ConA. A possible reason to explain this phenomenon is, the BSA provides a 3D scaffold for mannose probe immobilization and subsequent capture of ConA.

Nonspecific binding of proteins is known to reduce the selectivity of various SPR-based biosensors. In order to verify that the SPR chip prepared with BSA-Man conjugate has the specificity only to ConA rather than other proteins, another lectin PNA (i.e, peanut agglutinin, which binds specifically with galactose and lactose) was investigated. Figure 3 shows the SPR kinetic data after injecting the same concentration (i.e., 10 μM) of PNA and ConA to a sensor prepared with BSA-M11. One can find that, when compared with ConA, the binding of PNA with BSA-M11 is negligible. This clearly indicates that the current sensor has very good specificity and could resist non-specific adsorption.

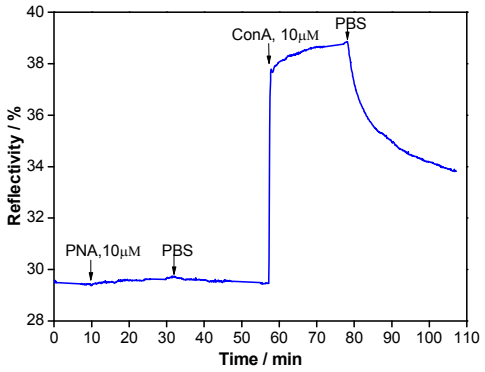

Figure 3. Comparison of the binding of two lectins (i.e., PNA and ConA) with the BSA-M11 as measured by SPR.

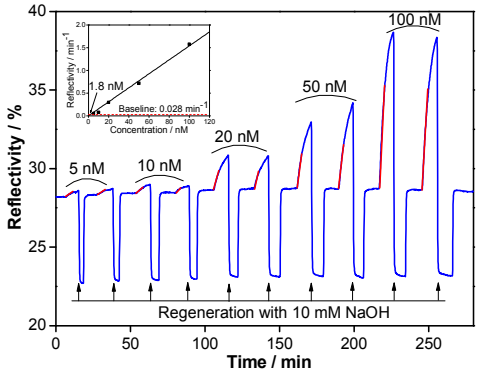

Figure 4. SPR kinetic measurements for the binding of ConA with concentration ranging from 5 to 100 nM. The SPR chip was prepared with BSA-M11.

In order to identify the limit of detection (LOD) of the present sensor, a series of ConA solutions ranging from 5 to 100 nM were tested sequentially with a chip prepared with BSA-M11, as shown in Figure 4. At such low concentrations, the initial binding process is controlled by the diffusion of ConA from the bulk to the surface, showing a linear signal increase with time. The slope of the SPR reflectivity increase is proportional to the ConA concentration. A calibration curve is thus obtained by plotting the measured slopes versus the ConA concentration (see the inset in Figure 4). The LOD is reached if the calibration curve intersects with the stability baseline. The baseline is defined as three times the standard deviation of the measurements of the time-dependent reflectivity without any ConA, which is about

0.028 min^{-1}. From the inset of Figure 4, it can be seen that the LOD of the current biosensor is 1.8 nM.

In summary, we demonstrated the synthesis of BSA-sugar conjugates with different mannose number ranging from 8 to 13. All conjugates could adsorb spontaneously onto the gold substrate without any surface modification, and could be employed for the detection of ConA with a LOD of 1.8 nM. SPR measurements showed that the optimized number of mannose probes under the current condition is 11, as manifested by the fast binding kinetics and the high affinity with ConA. Therefore, these new BSA-based conjugates allow for a straightforward and effective strategy for the fabrication of glycan biosensors. Considering the fact that BSA can adsorb onto many surface of different materials (i.e., metals, polymers, ceramics, etc.) and is widely used as blocking agent to reduce the non-specific protein adsorption, we anticipate that the current immobilization strategy is useful not only for the biosensors consisting of small sugar probes, but also promising for the fabrication of various biomedical devices, such as cell culture scaffolds, affinity chromagraphy, separation membrane, etc.

ASSOCIATED CONTENT

Supporting Information.

Experimental details, including materials, synthesis and characterization of the derived mannoses and BSA-sugar conjugates, SPR anslysis, etc. The Supporting Information is available free of charge on the ACS Publications website.

AUTHOR INFORMATION

Corresponding Author

* Tel: +86 22 60602476; Fax: +86 22 60602430; E-mail: chuliqiang@tust.edu.cn (L.-Q. Chu); yyang@tust.edu.cn (Y. Yang)

ACKNOWLEDGMENTS

The authors are grateful to the Program for New Century Excellent Talents in University (NCET-12-1064) and the Natural Science Foundation of China (21402140) for financial support.

REFERENCES

(1) Wang, S. K.; Cheng, C. M., Glycan-Based Diagnostic Devices: Current Progress, Challenges and Perspectives. *Chem. Commun.* **2015,** 51, 16750-16762.
(2) Hushegyi, A.; Tkac, J., Are Glycan Biosensors an Alternative to Glycan Microarrays? *Anal. Methods* **2014,** 6, 6610-6620.
(3) Mammen, M.; Choi, S. K.; Whitesides, G. M., Polyvalent Interactions in Biological Systems: Implications for Design and Use of Multivalent Ligands and Inhibitors. *Angew. Chem. Int. Ed.* **1998,** 37, 2755-2794.
(4) Donczo, B.; Kerekgyarto, J.; Szurmai, Z.; Guttman, A., Glycan Microarrays: New Angles and New Strategies. *Analyst* **2014,** 139, 2650-2657.
(5) Park, S.; Gildersleeve, J. C.; Blixt, O.; Shin, I., Carbohydrate Microarrays. *Chem. Soc. Rev.* **2013,** 42, 4310-4326.
(6) Penezic, A.; Deokar, G.; Vignaud, D.; Pichonat, E.; Happy, H.; Subramanian, P.; Gasparovic, B.; Boukherroub, R.; Szunerits, S., Carbohydrate-Lectin Interaction on Graphene-Coated Surface Plasmon Resonance (SPR) Interfaces. *Plasmonics* **2014,** 9, 677-683.
(7) Maalouli, N.; Barras, A.; Siriwardena, A.; Bouazaoui, M.; Boukherroub, R.; Szunerits, S., Comparison of Photo- and Cu(I)-Catalyzed "Click" Chemistries for the Formation of Carbohydrate SPR Interfaces. *Analyst* **2013,** 138, 805-812.
(8) Scheicher, S. R.; Kainz, B.; Köstler, S.; Reitinger, N.; Steiner, N.; Ditlbacher, H.; Leitner, A.; Pum, D.; Sleytr, U. B.; Ribitsch, V., 2D Crystalline Protein Layers as Immobilization Matrices for the Development of DNA Microarrays. *Biosens. Bioelectron.* **2013,** 40, 32-37.
(9) Coad, B. R.; Vasilev, K.; Diener, K. R.; Hayball, J. D.; Short, R. D.; Griesser, H. J., Immobilized Streptavidin Gradients as Bioconjugation Platforms. *Langmuir* **2012,** 28, 2710-2717.
(10) Huang, B. X.; Kim, H.-Y.; Dass, C., Probing Three-Dimensional Structure of Bovine Serum Albumin by Chemical Cross-linking and Mass Spectrometry. *J. Am. Soc. Mass Spectrom.* **2004,** 15, 1237-1247.
(11) Pai, J.; Hyun, J. Y.; Jeong, J.; Loh, S.; Cho, E. H.; Kang, Y. S.; Shin, I., Carbohydrate Microarrays for Screening Functional Glycans. *Chemical Science* **2016,** 7, 2084-2093.
(12) Clausen, M.; Madsen, R., Synthesis of Oligogalacturonates Conjugated to BSA. *Carbohydr. Res.* **2004,** 339, 2159-2169.
(13) Oyelaran, O.; Li, Q.; Farnsworth, D.; Gildersleeve, J. C., Microarrays with Varying Carbohydrate Density Reveal Distinct Subpopulations of Serum Antibodies. *J. Proteome Res.* **2009,** 8, 3529-3538.
(14) Gildersleeve, J. C.; Oyelaran, O.; Simpson, J. T.; Allred, B., Improved Procedure for Direct Coupling of Carbohydrates to Proteins via Reductive Amination. *Bioconjugate Chem.* **2008,** 19, 1485-1490.
(15) Willats, W. G. T.; Rasmussen, S. E.; Kristensen, T.; Mikkelsen, J. D.; Knox, J. P., Sugar-Coated Microarrays: A Novel Slide Surface for the High-Throughput Analysis of Glycans. *Proteomics* **2002,** 2, 1666-1671.
(16) Yonzon, C. R.; Jeoungf, E.; Zou, S. L.; Schatz, G. C.; Mrksich, M.; Van Duyne, R. P., A Comparative Analysis of Localized and Propagating Surface Plasmon Resonance Sensors: The Binding of Concanavalin a to a Monosaccharide Functionalized Self-Assembled Monolayer. *J. Am. Chem. Soc.* **2004,** 126, 12669-12676.
(17) Wurm, F.; Steinbach, T.; Klok, H. A., One-Pot Squaric Acid Diester Mediated Aqueous Protein Conjugation. *Chem. Commun.* **2013,** 49, 7815-7817.
(18) Jachimska, B.; Tokarczyk, K.; Lapczynska, M.; Puciul-Malinowska, A.; Zapotoczny, S., Structure of Bovine Serum Albumin Adsorbed on Silica Investigated by Quartz Crystal Microbalance. *Colloids Surf., A* **2016,** 489, 163-172.
(19) Figueira, V. B. C.; Jones, J. P., Viscoelastic Study of the Adsorption of Bovine Serum Albumin on Gold and Its Dependence on pH. *J. Colloid Interface Sci.* **2008,** 325, 107-113.
(20) Norde, W.; Anusiem, A. C. I., Adsorption, Desorption and Re-adsorption of Proteins on Solid Surfaces. *Colloids Surf.* **1992,** 66, 73-80.
(21) Knoll, W., Interfaces and Thin Films as Seen by Bound Electromagnetic Waves. *Annu. Rev. Phys. Chem.* **1998,** 49, 569-638.
(22) Jung, L. S.; Campbell, C. T.; Chinowsky, T. M.; Mar, M. N.; Yee, S. S., Quantitative Interpretation of the Response of Surface Plasmon Resonance Sensors to Adsorbed Films. *Langmuir* **1998,** 14, 5636-5648.
(23) Chu, L.-Q.; Knoll, W.; Forch, R., Pulsed Plasma Polymerized Di(ethylene glycol) Monovinyl Ether Coatings for Nonfouling Surfaces. *Chem. Mater.* **2006,** 18, 4840-4844.
(24) Voros, J., The Density and Refractive Index of Adsorbing Protein Layers. *Biophys. J.* **2004,** 87, 553-561.
(25) Safina, G., Application of Surface Plasmon Resonance for the Detection of Carbohydrates, Glycoconjugates, and Measurement of the Carbohydrate-Specific Interactions: A Comparison with Conventional Analytical Techniques. A Critical Review. *Anal. Chim. Acta* **2012,** 712, 9-29.
(26) Duverger, E.; Frison, N.; Roche, A. C.; Monsigny, M., Carbohydrate-Lectin Interactions Assessed by Surface Plasmon Resonance. *Biochimie* **2003,** 85, 167-179.
(27) Munoz, E. M.; Correa, J.; Riguera, R.; Fernandez-Megia, E., Real-Time Evaluation of Binding Mechanisms in Multivalent Interactions: A Surface Plasmon Resonance Kinetic Approach. *J. Am. Chem. Soc.* **2013,** 135, 5966-5969.
(28) Smith, E. A.; Thomas, W. D.; Kiessling, L. L.; Corn, R. M., Surface Plasmon Resonance Imaging Studies of Protein-Carbohydrate Interactions. *J. Am. Chem. Soc.* **2003,** 125, 6140-6148.
(29) Becker, J. W.; Reeke, G. N.; Wang, J. L.; Cunningham, B. A.; Edelman, G. M., The Covalent and Three-Dimensional Structure of Concanavalin A. III. Structure of the Monomer and Its Interactions with Metals and Saccharides. *J. Biol. Chem.* **1975,** 250, 1513-1524.

For the Table of Contents (TOC)

BSA-Sugar Conjugates as Ideal Building Blocks for SPR-Based Glycan Biosensors